Available online at www.sciencedirect.com

SCIENCE DIRECT

Developmental Biology 278 (2005) 440–458

DEVELOPMENTAL BIOLOGY

www.elsevier.com/locate/ydbio

Extensive and orderly reprogramming of genome-wide chromatin modifications associated with specification and early development of germ cells in mice

Yoshiyuki Seki[a,b,c,d,*], Katsuhiko Hayashi[a,c], Kunihiko Itoh[e], Michinao Mizugaki[f], Mitinori Saitou[d,g,h], Yasuhisa Matsui[a,b,c,i]

[a]*Department of Molecular Embryology, Research Institute, Osaka Medical Center for Maternal and Child Health, Murodo-cho 840, Izumi, Osaka 594-1101, Japan*

[b]*Graduate School of Medicine, Osaka University, 3-1 Yamada-oka, Suita, Osaka 565-0871, Japan*

[c]*CREST, Japan Science and Technology Agency, 4-1-8 Honmachi, Kawaguchi, Saitama 332-0012, Japan*

[d]*Laboratory for Mammalian Germ Cell Biology, Center for Developmental Biology, RIKEN Kobe Institute, 2-2-3 Minatojima-Minamimachi, Chuo-ku, Kobe 650-0047, Japan*

[e]*Department of Pharmaceutical Science, Akita University Hospital, 1-1-1 Hondo, Akita 010-8543, Japan*

[f]*Department of Clinical Pharmaceutics, Tohoku Pharmaceutical University, 4-4-1 Komatsuhima, Aoba-ku, Sendai 981-8558, Japan*

[g]*Precursory Research for Embryonic Science and Technology, Japan Science and Technology Agency, 4-1-8 Honmachi, Kawaguchi, Saitama 332-0012, Japan*

[h]*Laboratory of Molecular Cell Biology and Development, Graduate School of Biostudies, Kyoto University, Oiwake-cho, Kitashirakawa, Sakyo-ku, Kyoto 606-8502, Japan*

[i]*Cell Resource Center for Biomedical Research, Institute of Development, Aging and Cancer, Tohoku University, 4-1 Seiryo-cho, Aoba-ku, Sendai 980-8575, Japan*

Received for publication 17 August 2004, accepted 18 November 2004
Available online 18 December 2004

Abstract

Induction of mouse germ cells occurs from the proximal epiblast at around embryonic day (E) 7.0. These germ cells then migrate to, and enter the gonads at about E10.5 after which they undergo epigenetic reprogramming including erasure of parental imprints. However, the epigenetic properties acquired by nascent germ cells and the potential remodeling of these epigenetic marks in the subsequent migratory period have been largely unexplored. Here we have used immunohistochemistry to examine several genome-wide epigenetic modifications occurring in germ cells from their specification to their colonization of the genital ridges. We show that at around E8.0, germ cells concomitantly and significantly reduce H3-K9 dimethylation and DNA methylation, two major repressive modifications for gene expression. These events are preceded by the transient loss of all the DNA methyltransferases from their nuclei. By contrast, germ cells substantially increase the levels of H3-K27 trimethylation, another repressive modification with more plasticity, at E8.5–9.0 and maintain this state until at least E12.5. H3-K4 methylation and H3-K9 acetylation, modifications associated with transcriptionally permissive/active chromatin, are similar in germ and surrounding somatic cells but germ cells transiently increase these marks sharply upon their entry into the genital ridge. H3-K9 trimethylation, a hallmark of centromeric heterochromatin, is kept relatively constant during the periods examined. We suggest that this orderly and extensive epigenetic reprogramming in premigratory and migratory germ cells might be necessary for their reacquisition of underlying totipotency, for subsequent specific epigenetic remodeling, including the resetting of parental imprints, and for the production of gametes with an appropriate epigenotype for supporting normal development.

Keywords: Germ cells; Epigenetics; Histone modification; DNA methylation; Reprogramming; Transcriptional repression

* Corresponding author. Laboratory for Mammalian Germ Cell Biology, Center for Developmental Biology, RIKEN Kobe Institute, 2-2-3 Minatojima-minamimachi, Chuo-ku, Kobe, 650-0047, Japan. Fax: +81 78 306 3377.
E-mail address: yseki@cdb.riken.jp (Y. Seki).

0012-1606/$ - see front matter © 2004 Elsevier Inc. All rights reserved.
doi:10.1016/j.ydbio.2004.11.025

Introduction

Germ line cells are exclusively programmed for the creation of a new organism, allowing transmission of original genetic information across generations. The unique capacity of germ cells to fulfill this function relies on their innate epigenetic reprogramming ability and their maintenance of underlying genomic totipotency (Surani, 2001). This is particularly challenging in mammals in which the germ line is derived from epiblast cells and is not predetermined at fertilization as in many other organisms (Saitou et al., 2003). In mice, the germ line epigenome seems to be remodeled in a temporally and spatially controlled manner throughout its development, which ultimately leads to the formation of haploid gametes that upon fusion initiate a new life. Perturbation of these processes leads to abnormal embryonic development, demonstrating the importance of epigenetic reprogramming in the germ line (Li, 2002). However, the precise mechanisms regulating these processes remain largely unknown.

Methylation of cytosine on the CpG dinucleotide is a key epigenetic modification involved in the imposition of differential epigenetic states on the genome, functionally associated with parental imprints, control of gene expression and genome structure (Bird, 2002). Generally, methylated DNA acts as a repressive element for transcription by creating a local heterochromatic structure (Li, 2002). CpG methylation is highly concentrated at centromeric heterochromatin and widely distributed throughout repressed regions within euchromatin. DNA methyltransferases (Dnmts: Dnmt1, Dnmt3a, Dnmt3b) are differentially responsible for establishing and maintaining methyl-CpG and disruption of these genes significantly perturbs genome-wide DNA methylation patterns, leading to aberrant development of homozygously null animals (Li et al., 1992; Okano et al., 1999). Remarkably, recent molecular, biochemical and genetic studies have identified another major epigenetic determinant of gene expression, i.e., the covalent modification of specific residues of histone N terminal tails (Jenuwein and Allis, 2001). These modifications include acetylation, phosphorylation, methylation, ubiquitination, and ADP ribosylation. Amongst these, methylation of lysine (K) residues of histone H3 has been shown to be important in the creation of distinct chromatin domains and a family of enzymes that have SET (Suv39, Enhancer of zeste, Trithorax) domains responsible for histone methyltransferase (HMTase) activity has been identified (Lachner et al., 2003). In general, dimethylation of H3-K9 mediated by G9a is associated with repressed genes/regions in euchromatin, and trimethylation of H3-K9 by Suv39h is concentrated at centromeric heterochromatin (Peters et al., 2001, 2003; Tachibana et al., 2002). In contrast, methylation of H3-K4 and acetylation of H3-K9 represent transcriptionally active/permissive chromatin (Jenuwein and Allis, 2001). Enhancer of zeste 2 (Ezh2) catalyzes repressive H3-K27 trimethylation on the inactive X chromosome and is also required for the derivation and propagation of embryonic stem (ES) cells (O'Carroll et al., 2001; Plath et al., 2003; Silva et al., 2003). H3-K27 trimethylation is thus reasoned to be important for the epigenetic plasticity of the pluripotent ES cell genome. Importantly, it has been reported that disruption of H3-K9 methylation in *Neurospora* abolishes DNA methylation as well, indicating a mechanistic interplay between these two key epigenetic marks (Tamaru and Selker, 2001). By contrast, in some cases, methylated DNA acts as a core element to recruit histone modification complexes (Hashimshony et al., 2003), and a mutation of a DNA methyltransferase in *Arabidopsis* resulted in the reduced levels of H3-K9 dimethylation (Soppe et al., 2002). Combined these findings point to a presence of complex molecular network that determines certain epigenetic states of particular cell types.

Early development in mammals culminates in the establishment of a blastocyst that consists of extraembryonic trophectoderm and pluripotent epiblast, from which all the somatic cell lineages as well as the germ line arise. Upon fertilization, the paternal genome is known to undergo active genome-wide DNA demethylation that is followed by passive replication-dependent demethylation of both the paternal and maternal genomes after the 2-cell stage, which continues until the morula stage, by which time the genome-wide DNA methylation level is very low (Li, 2002; Mayer et al., 2000; Oswald et al., 2000; Rougier et al., 1998). Genome-wide H3-K9 dimethylation decreases in a similar manner, reaching its lowest state at the 8-cell stage (Arney et al., 2002; Liu et al., 2004). Thereafter, in the pluripotent epiblast, Dnmt3a and 3b become active and the methylation levels in the epiblast cells increase rapidly (Li, 2002; Watanabe et al., 2002). Germ cells in mice are recruited from the proximal epiblast cells in response to signaling molecules at around embryonic day (E) 7.0 (Ginsburg et al., 1990; Lawson and Hage, 1994; Lawson et al., 1999; Saitou et al., 2002). Established germ cells start to migrate in the hindgut and mesentery (Anderson et al., 2000), eventually colonizing the differentiating genital ridges after E10.5. Between E10.5 and E12.5, germ cells undergo unique and extensive epigenetic reprogramming which appears to be equivalent in both sexes (Hajkova et al., 2002; Molyneaux et al., 2001; Sato et al., 2003; Tam et al., 1994). This reprogramming includes the erasure of parental imprints, reactivation of inactive X chromosome, and genome-wide CpG demethylation. However, the precise cellular and molecular mechanisms involved in these events remain largely obscure. Moreover, epigenetic properties that germ cells initially acquire upon specification and their potential remodeling in the migratory stage have been poorly resolved.

To address these issues, we have explored genome-wide epigenetic modifications in mouse germ cells from their specification to their entry into genital ridges using whole mount immunohistochemistry. Our data show that in germ cells the level of H3-K9 dimethylation decreases greatly at around E8.0, and is temporally closely coupled to genome-

wide demethylation of DNA. By contrast, H3-K27 trimethylation is strongly enhanced from E8.5. The H3-K4 methylation and H3-K9 acetylation levels are comparable in migrating germ cells and surrounding somatic cells but germ cells sharply up-regulate both modifications at E10.5, coincident with their colonization of the genital ridges. We

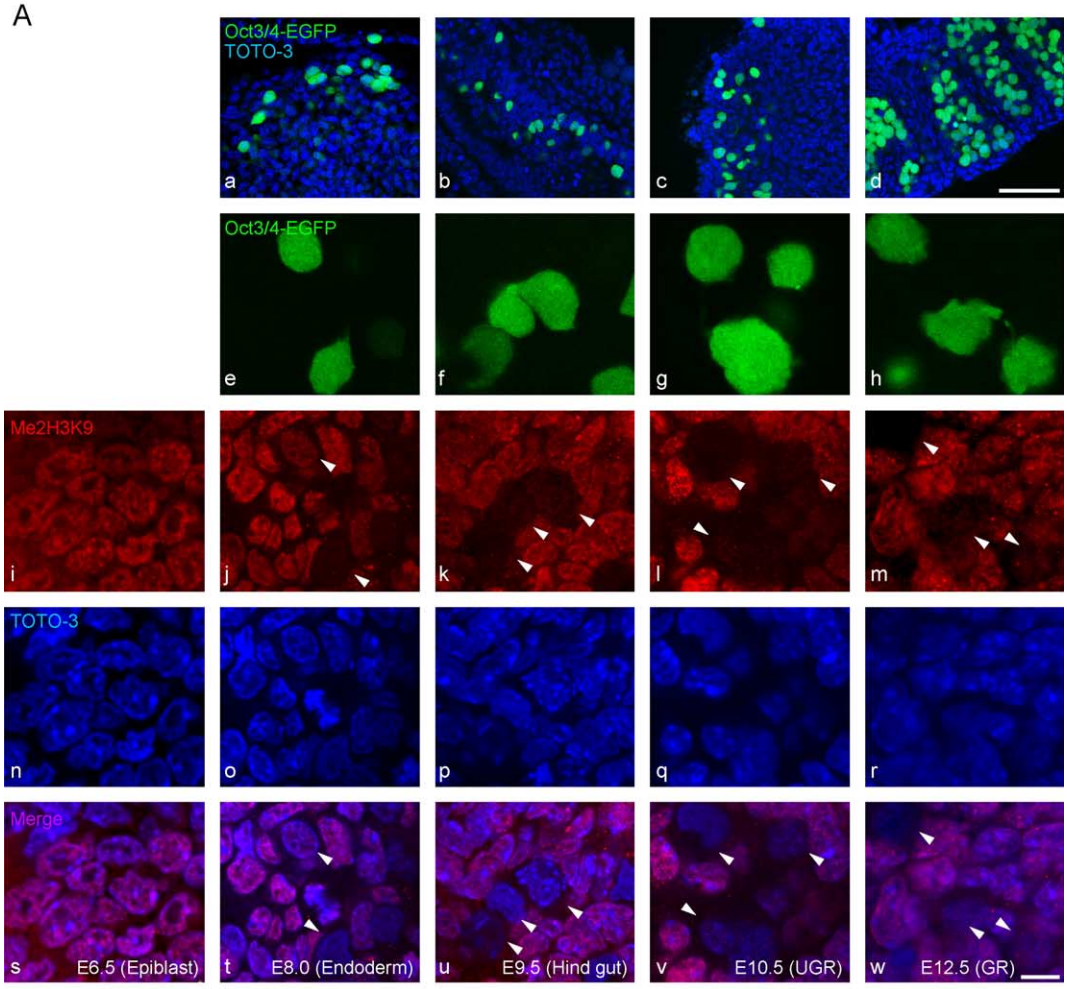

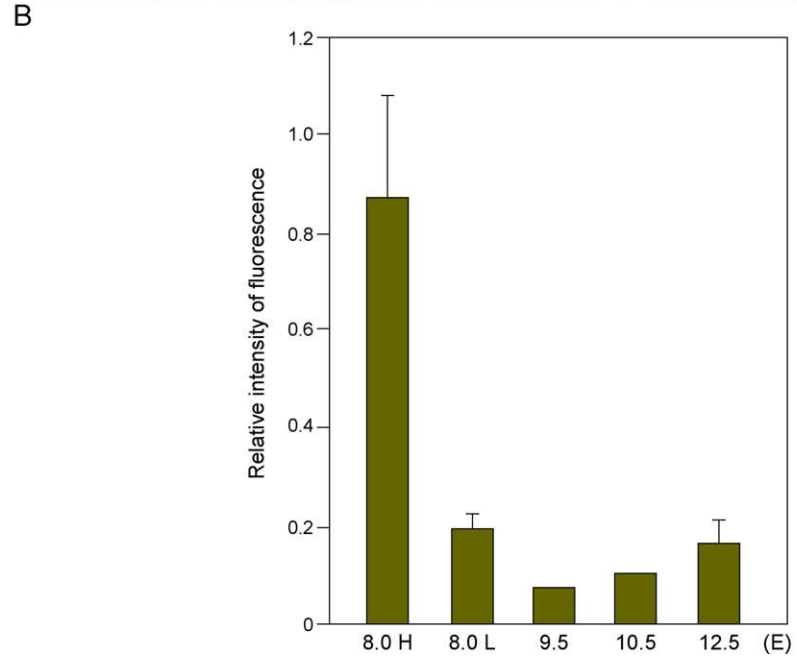

suggest that this extensive epigenetic reprogramming in early germ cells is necessary to maintain their underlying totipotency and might be prerequisite for subsequent specific epigenetic remodeling, including the erasure and re-addition of parental imprints. This complex germ-cell-specific epigenetic program is probably critical for appropriate germ line development, which is ultimately required for the successful development of a new generation.

Materials and methods

Antibodies

The following antibodies were used at the indicated dilution, and were obtained from indicated sources: rabbit anti-dimethylated histone H3-K9 (1/500, Upstate); rabbit anti-trimethyl histone H3-K9 (1/500, Upstate); rabbit anti-trimethyl histone H3-K27 (1/500, Upstate); mouse anti-HP1 alpha (1/500, Chemicon); rabbit anti-acetylated H3-K9 (1/500, Upstate); rabbit anti-methylated H3-K4 (1/500, Upstate); mouse anti-beta-actin (1/5000, Abcam). Rabbit anti-Stella antibody was described previously (Saitou et al., 2002). The following antibodies were kindly provided by Dr. Shoji Tajima and Dr. Isao Suetake, University of Osaka, and were used at the indicated dilution: rabbit anti-Dnmt1 (1/500), rabbit anti-Dnmt3a (1/500), and rabbit anti-Dnmt3b (1/500). Mouse anti-methylated cytosine antibody (Sakai et al., 2001) was used at a 1/100 dilution. Secondary antibodies purchased from Molecular Probes were used at a 1/500 dilution. These secondary antibodies were Alexa Fluor™ 568 goat anti-rabbit IgG, Alexa Fluor™ 568 goat anti-mouse IgG and Alexa Fluor™ 568 goat anti-mouse IgM.

Whole-mount immunofluorescence staining

Female ICR mice mated with male transgenic mice of the GOF-18/deltaPE/GFP line were sacrificed at appropriate stages (E7.0–12.5) to recover embryos. Embryos were washed with PBS containing 0.1% BSA (SIGMA), fixed in 4% paraformaldehyde and then subjected to three 15-min washes with PBST (PBS containing 0.05% Tween-20). The embryos were incubated with primary antibodies in PBS containing 5% skim milk and 1% Triton X-100 for 48 h at 4°C. Embryos were then subjected to three 4-h washes with PBST, and incubated with the Alexa Fluor 568 secondary antibody in PBS containing 0.1% BSA and 1% Triton X-100 and a 1/2500 dilution of TOTO-3 (Molecular Probes) containing 100 μg/ml of RNase A for 24 h at 4°C. The embryos were subjected to three 4-h washes with PBST for 4 h, mounted on cover slips and observed under a confocal laser microscope (Leica). For the methylated cytosine antibody reaction, the embryos were treated with 100 μg/ml RNase A in 2× SSC for 3 h at room temperature and treated with 2 N HCl for 3 h.

Single-cell immunofluorescence staining

E12.5 genital ridges and E9.5 hindgut were washed with PBS and treated with 0.05% trypsin/EDTA for 10 min at 37°C. The resulting cell suspensions were put on poly-L-lysine-coated glass slides and fixed with 4% paraformaldehyde for 15 min at 4°C. The cells were permeabilized and denatured for 1 h in 2 N HCl. After washing with PBS, the cells were subsequently double stained with anti-Stella and methylated cytosine antibodies. Then, the cells were washed with PBS and incubated with secondary antibody containing 100 μg/ml of Rnase and a 1/2500 dilution of TOTO-3 for 1 h.

Quantification of fluorescence intensity by laser-scanning confocal microscopy

Fluorescence was detected using nonsaturating conditions on a laser-scanning confocal microscope (Leica) and the signal was quantified using an NIH-Image (National Institutes of Health, Bethesda, MD) as follows. The average nucleus pixel value/unit area was subtracted from the average cytoplasmic pixel value/unit. The average value of about 10 surrounding somatic cells was set as 1, and the average fluorescence intensity of 10 germ cells was indicated relative to this value with an error bar.

Western blotting

Genital ridges at E12.5 were dissected and dissociated in 0.25% trypsin for 15 min at 37°C. The resulting cell suspension was filtrated through a nylon mesh and sorted using an EPICS ALTRA flow cytometer. GFP-positive and -negative cells were lysed by SDS sample buffer (50 mM Tris–HCl, 2% SDS, 10% Glycerol pH 6.8). Alternatively, germ cells were enriched by magnetic immunoaffinity isolation using antibodies against stage-specific embryonic antigen 1 as described (Pesce and De Felici, 1995). The resulting populations of germ cells were around 90% pure,

Fig. 1. H3-K9 dimethylation states in developing germ cells compared to those in surrounding somatic cells. The levels of H3-K9 dimethylation are significantly reduced in germ cells at E8.0, and remain low until E12.5. Oct4ΔPE:GFP$^+$ transgenic embryos at E6.5 (i, n, s), 8.0 (a, e, j, o, t), 9.5 (b, f, k, p, u), 10.5 (c, g, l, q, v), 12.5 (d, h, m, r, w) stained with anti-dimethylated H3-K9 antibody (red) and TOTO-3 (blue). GFP-positive cells (green) represent germ cells. More than 10 images were obtained at each stage and representative examples are shown. (a–d) Localization of germ cells at E8.0, 9.5, 10.5, and 12.5, respectively, visualized by EGFP, (e–h) high magnification of images a–d, which were doubly stained with anti-dimethylated H3-K9 (j–m) and TOTO-3 (o–r). Epiblast cells at E6.5, which were all positive for Oct4, were doubly stained with anti-dimethylated H3-K9 (i) and TOTO-3 (n). (s–w) Merged images of H3-K9 dimethylation and TOTO-3 staining. Arrowheads indicate germ cells. Scale bar in (d), 100 μm, in (w) 10 μm. (B) Semiquantification of H3-K9 dimethylation levels in developing germ cells compared to those in neighboring somatic cells. The intensity of fluorescent signals was quantified as described in Materials and methods. The average value for 10 somatic cells at each stage was set as 1.0. At E8.0, germ cells showed either high (8.0 H) or low (8.0 L) dimethylated H3-K9 levels.

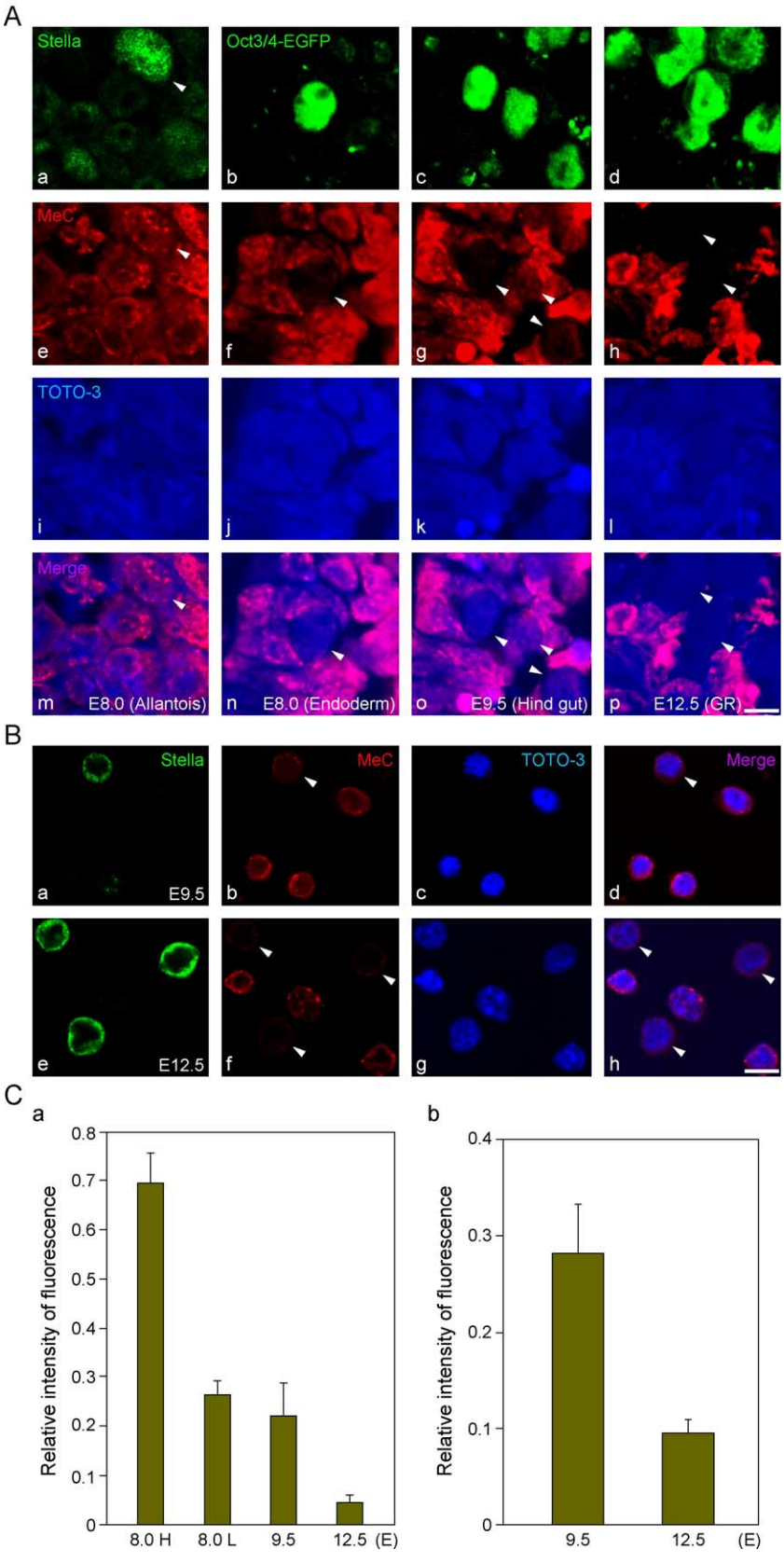
A
Stella
Oct3/4-EGFP
MeC
TOTO-3
Merge
a
b
c
d
e
f
g
h
i
j
k
l
m E8.0 (Allantois)
n E8.0 (Endoderm)
o E9.5 (Hind gut)
p E12.5 (GR)
B
Stella
MeC
TOTO-3
Merge
a E9.5
b
c
d
e E12.5
f
g
h
C
a
Relative intensity of fluorescence
0
0.1
0.2
0.3
0.4
0.5
0.6
0.7
0.8
8.0 H
8.0 L
9.5
12.5 (E)
b
Relative intensity of fluorescence
0
0.1
0.2
0.3
0.4
9.5
12.5
(E)

judged by immunofluorescence using anti-Stella antibody. Proteins were separated on NuPAGE™ 10% Bis–Tris gel (Invitrogen), and blotted onto Immobilion transfer membrane (Millipore). The primary antibody reactions were performed according to standard protocols. Primary antibodies were detected with anti-mouse-HRP or anti-rabbit HRP (Jackson Immunoresearch) followed by ECL advance detection.

Results

To examine genome-wide chromatin modification states of developing germ cells, we exploited whole-mount immunohistochemistry combined with confocal microscopic analysis, as this approach would allow direct comparison of chromatin states of germ cells with those of neighboring somatic cells. Since germ cells and surrounding somatic cells share common precursors, comparison of these cells might provide important information regarding the events associated with germ line specification. We used embryos from Oct4 del PE: EGFP transgenic mice to specifically locate germ cells after E7.5 (Yoshimizu et al., 1999).

H3-K9 dimethylation is substantially down-regulated in germ cells at around E8.0

Firstly, the distribution of H3-K9 dimethylation was examined. It has been reported that dimethylated H3-K9 mainly associates with repressed genes/regions on euchromatic arms and, to a lesser extent, with centromeric heterochromatin of interphase nuclei (Peters et al., 2003). Proximal epiblast cells, from which both germ cells and extraembryonic mesodermal cells arise, showed dispersed dimethyl H3-K9 staining with many small foci in their nuclei (Fig. 1Ai). Consistent with previous studies, the majority of these foci did not co-localize with TOTO-3-positive centromeric heterochromatin (Fig. 1An,s), suggesting that these foci are on the euchromatic arms. The nucleoli were devoid of the staining. We could not observe any distinct cell types judging from the distribution of H3-K9 dimethylation at this stage. At E8.0, germ cells were specifically identified with bright EGFP signals driven by a distal promoter of *Oct4* (Fig. 1Aa,e) (Yoshimizu et al., 1999). The somatic hindgut endoderm surrounding migrating germ cells exhibited relatively uniform signals (Fig. 1Aj), the distribution of which looked similar to those in other somatic cells in the same embryos (data not shown). By contrast, we observed that GFP-positive germ cells showed heterogeneous H3-K9 dimethylation signal intensities, which were either relatively strong and comparable to those in neighboring somatic cells, or very weak (Fig. 1Aj). When we semiquantitatively measured the fluorescent intensities (see Materials and methods), germ cells at this stage were clearly found to exhibit either high or low intensities (Fig. 1B). The signal distributions in germ cells showing higher fluorescence were similar to those in surrounding somatic cells. From E9.5 to E12.5, GFP-positive germ cells consistently exhibited very low signals, with lowest relative intensities at E9.5 (Figs. 1Ak–m,B). The low staining in germ cells was not due to the specific inaccessibility of the antibody to the germ cell nuclei, as other antibodies against different histone modifications demonstrated clear signals (see below). These findings therefore suggest that germ cells actively remove the majority of H3-K9 dimethylation at around E8.0, and then maintain a constant low level until at least E12.5.

Genome-wide demethylation of DNA temporally couples to demethylation of H3-K9

Germ cells have been reported to erase DNA methylation of imprinted genes and some single copy genes after their entry into genital ridges (Hajkova et al., 2002; Sato et al., 2003). Centromeric LINE1-repeated sequences were also shown to demethylate but IAP elements were found to be more resistant (Lane et al., 2003). However, little is known about the methylation status of other highly and mildly repeated sequences, which, due to their high GC content, may have a significant impact on the overall level of genome methylation (Sanford et al., 1984; Yoder et al., 1997).

Fig. 2. Genome-wide DNA methylation states in developing germ cells compared to those in surrounding somatic cells. Germ cell genome is substantially demethylated at around E8.0. Oct4ΔPE:GFP^{+} transgenic embryos at E8.0 (b, f, j, n), 9.5 (c, g, k, o), 12.5 (d, h, l, p) were stained with anti-methylcytosine antibody (red) and TOTO-3 (blue). GFP-positive cells (green) represent germ cells. Germ cells at the base of allantois were also stained with anti-Stella antibody (a). These E8.0 pre-migratory germ cells retained DNA methylation levels similar to neighboring somatic cells (a, e, m), while E8.0 germ cells already migrating in the endoderm had lost their DNA methylation (b, f, n). More than 10 images were obtained at each stage and representative examples are shown. (m–p) Merged images of methylated cytosine and TOTO-3 staining. Embryos had to be treated with HCl and RNase for a long time to expose the methylated cytosine as an antigen (see Materials and methods), which resulted in rather diffuse staining of TOTO-3. Arrowheads point to germ cells. Scale bar in (p), 10 μm. Dissociated germ cells and somatic cells were stained with anti-Stella antibody (a, e), anti-methylcytosine antibody (b, f), and TOTO-3 (c, g). (d, h) Shows merged images of methylated cytosine and TOTO-3 staining. (a–d) Represents cells from E9.5 and (e–h) represents cells from E12.5. Arrowheads point to germ cells. Scale bar in (h), 10 μm. Semiquantification of methylated cytosine levels in developing germ cells compared to those in neighboring somatic cells; (a) shows quantification from whole-mount staining and (b) from single cell staining. The intensity of fluorescent signals was quantified as described in Materials and methods. The average value for 10 somatic cells at each stage was set as 1.0. At E8.0, germ cells showed either high (8.0 H) or low (8.0 L) DNA methylation levels. At E12.5, DNA methylation levels were further down-regulated. Note that the timing of DNA demethylation at E8.0 coincides with that of demethylation of dimethylated H3-K9.

These sequences include major satellite sequences within mouse centromeres and the SINES. To analyze genome-wide DNA methylation changes during germ cell development, we stained embryos with an anti 5-methyl cytosine antibody. At E8.0, extraembryonic mesodermal somatic cells displayed several highly stained perinuclear foci, highlighted against an overall lower nuclear signal (Fig. 2Ae). Germ cells surrounded by these cells at the base of allantois showed similar distribution and intensity of the fluorescent signal (Fig. 2Aa,e), indicating that the genome-wide DNA methylation level is comparable between germ and somatic cells at this stage. However, in embryos of a similar developmental stage, germ cells already migrating in the hindgut endoderm showed significantly reduced signal intensities (Fig. 2Ab,f). At E9.5, all the migrating germ cells exhibited low DNA methylation signals (Fig. 2c,g). These findings indicate that at about E8.0 CpG methylation is substantially removed from migrating germ cells. Significantly, the timing of DNA demethylation looked similar to that of demethylation of H3-K9 dimethylation, implying that a mechanistic link exists between these two events. By E12.5, when erasure of CpG methylation from imprinted genes has been reported to occur, the level of genome-wide DNA methylation appeared to be further down-regulated (Figs. 2Ad,h and Ca), a result that is consistent with the previous studies (Hajkova et al., 2002; Sato et al., 2003). To confirm these whole-mount staining data, we used the methyl cytosine antibody to stain E9.5 and E12.5 dissociated single germ cells that were attached on the same slide. This experiment confirmed that germ cells already had very low DNA methylation levels at E9.5 (Figs. 2B and Cb), which seemed to be further reduced by E12.5. These data, in combination with previous reports, suggest that germ cells undergo a minimum of two DNA demethylation processes, the first occurring at around E8.0 and affecting the bulk of the genome and the second occurring in the genital ridges at around E12.5, which results in imprint erasure.

Transient loss of all the Dnmts in germ cells precedes DNA demethylation

To gain some mechanistic insight into the DNA demethylation we observed in germ cells, the expression of three known DNA methyltransferases, Dnmt1, Dnmt3a, and Dnmt3b in germ cells was examined. Interestingly, we consistently found that the maintenance methyltransferase Dnmt1 was transiently down-regulated in germ cells located at the base of allantois at around E8.0 (Figs. 3Aa,f and Bf,j). Dnmt1 was expressed at earlier stages (Fig. 3Bb) and the absence of Dnmt1 from the germ cell nuclei lasts approximately for 16 h, which roughly corresponds to the cell cycle length of migratory germ cells (Tam and Snow, 1981). The de novo methyltransferase, Dnmt3b, was found to be absent from germ cell nuclei from soon after germ line specification until at least up to E12.5 (Figs. 3D,E). Dnmt3a showed consistently low-level expression in germ cells (Fig. 3C). These observations revealed that germ cells transiently lose all the known DNA methyltransferases at around E8.0 for about 16 h. Significantly, this loss of DNA methyltransferase activity coincides with the first round of DNA demethylation and loss of H3-K9 dimethylation that we observed in germ cells.

Specific up-regulation of H3-K27 trimethylation follows loss of H3-K9 dimethylation and DNA demethylation

We then went on to analyze another repressive modification, H3-K27 trimethylation, which is imposed by Ezh2 and is essential for the initiation of X chromosome inactivation and ES cell derivation from inner cell mass (O'Carroll et al., 2001; Plath et al., 2003; Silva et al., 2003). Ezh2 and its interacting partner embryonic ectoderm development (Eed) are the most highly conserved polycomb group (PcG) genes that are involved in heritable epigenetic regulation of gene expression, and the only known PcG members in *Caenorhabditis elegans*, where they are indispensable in

Fig. 3. Expression of Dnmts in developing germ cells compared to those in surrounding somatic cells. Germ cells lose all the Dnmts transiently at around E8.0. (A) Oct4ΔPE:GFP$^+$ transgenic embryos at E6.5 (e, j, o), 8.0 (a, f, k, p), 9.5 (b, g, l, q), 10.5 (c, h, m, r), and 12.5 (d, i, n, s) stained with anti-Dnmt1 antibody (red, e–i) and TOTO-3 (blue, j–n). GFP-positive cells (green, a–d) represent germ cells. Merged images of Dnmt1 and TOTO-3 staining are shown in (o–s). Note that Dnmt1 expression in germ cells at the base of allantois at E8.0 was barely detectable (a, f, p). Arrowheads indicate germ cells. Scale bar in (s), 10 μm. (B) Oct4ΔPE:GFP$^+$ transgenic embryos at E7.5 [early bud (EB) stage or late bud stage (LB)] stained with anti-Dnmt1 antibody (red, b, f, j) and TOTO-3 (blue, c, g, k). GFP strongly positive cells (green, a, e, i) most likely represent germ cells. Merged images of Dnmt1 and TOTO-3 staining are shown in (d, h, l). Note that presumptive germ cells at the EB stage retained Dnmt1 signal (a–d), which was substantially reduced at the LB stage (e–l). Arrowheads indicate germ cells. Scale bar in (h), 100 μm, in (l), 10 μm. (C) Oct4ΔPE:GFP$^+$ transgenic embryos at E6.5 (e, j, o), 8.0 (a, f, k, p), 9.5 (b, g, l, q), 10.5 (c, h, m, r), and 12.5 (d, i, n, s) stained with anti-Dnmt3a antibody (red, e–i) and TOTO-3 (blue, j–n). GFP-positive cells (green, a–d) represent germ cells. Merged images of Dnmt3a and TOTO-3 staining are shown in (o–s). Dnmt3a consistently showed low level or no expression in germ cells (e–i), whereas gonadal somatic cells exhibited substantial expression (h,i). Arrowheads indicate germ cells. Scale bar in (s), 10 μm. (D) Oct4ΔPE:GFP$^+$ transgenic embryos at E6.5 (e, j, o), 8.0 (a, f, k, p), 9.5 (b, g, l, q), 10.5 (c, h, m, r), and 12.5 (d, i, n, s) stained with anti-Dnmt3b antibody (red, e–i) and TOTO-3 (blue, j–n). GFP-positive cells (green, a–d) represent germ cells. Merged images of Dnmt3b and TOTO-3 staining are shown in (o–s). Dnmt3b consistently showed low level or no expression in germ cells (f–i), whereas somatic cells exhibited substantial expression especially at earlier stages (e,f). Germ cells in the genital ridge had Dnmt3b in their cytoplasm (h,i). Arrowheads indicate germ cells. Scale bar in (s), 10 μm. (E) Oct4ΔPE:GFP$^+$ transgenic embryos at E7.5 [early bud (EB)] stained with anti-Dnmt3b antibody (red, b, f) and TOTO-3 (blue, c, g). GFP strongly positive cluster of cells (green, a, e) represent most likely germ cells. Merged images of Dnmt3b and TOTO-3 staining are shown in (d, h). (e–h) are magnified images of (a–d), respectively. Dnmt3b was absent from germ cells as early as EB stage. Arrowheads indicate germ cells. Scale bar in (d), 100 μm, in (h), 10 μm.

the germ line gene silencing (Holdeman et al., 1998; Seydoux and Strome, 1999).

In the proximal epiblast cells, H3-K27 trimethylation was highly concentrated in large single spots within the nuclei that presumably mark the inactive X chromosome (Fig. 4Ae). The very strong fluorescent signal in these epiblast cells is consistent with the idea that random X inactivation has recently been initiated in these cells (Silva et al., 2003). At E8.0, hindgut somatic cells exhibited similar single accumulations of H3-K27 trimethylation but the fluorescent intensity appeared to be lower compared to that of epiblast cells (Fig. 4Aa,f). By contrast, GFP-

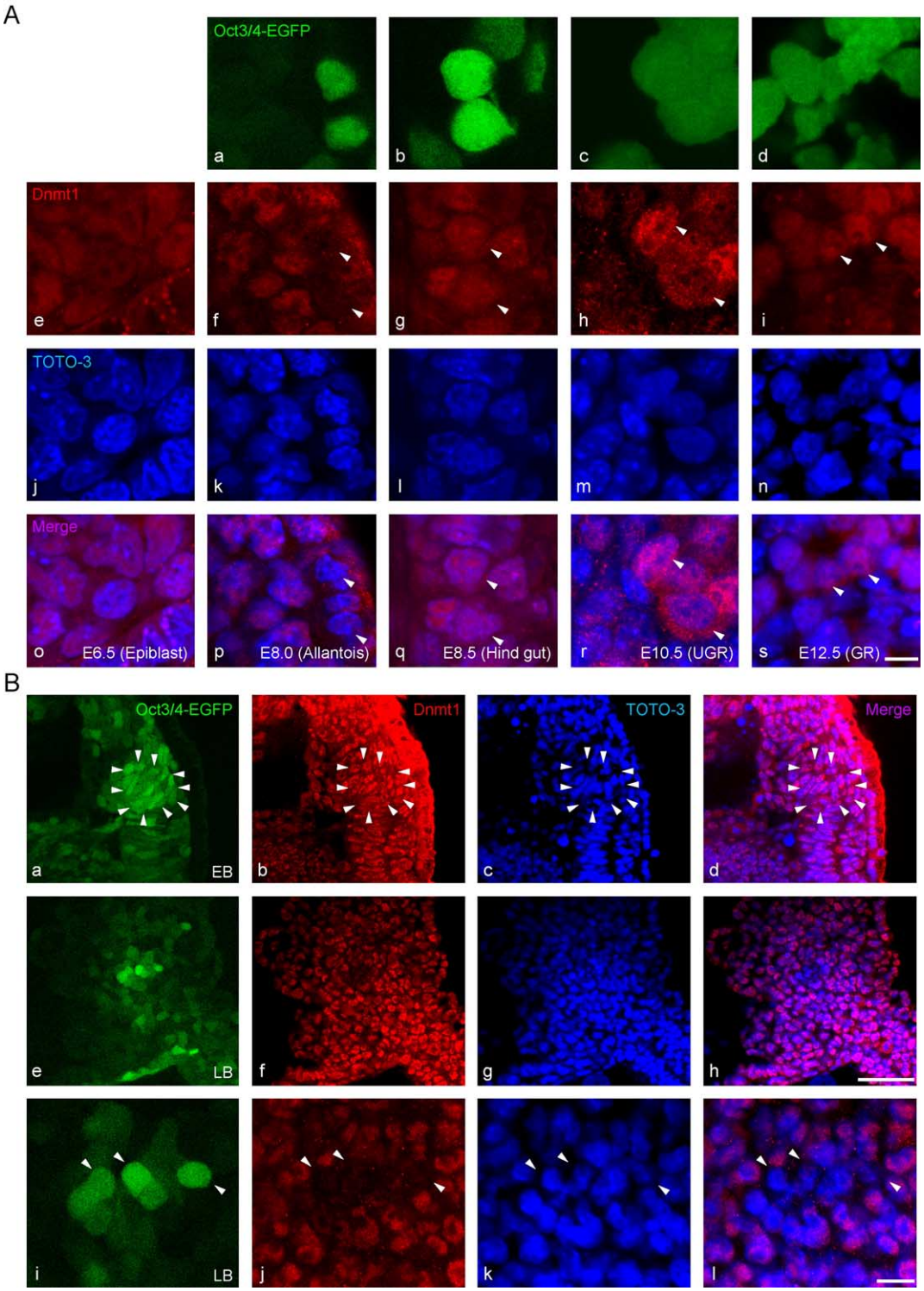

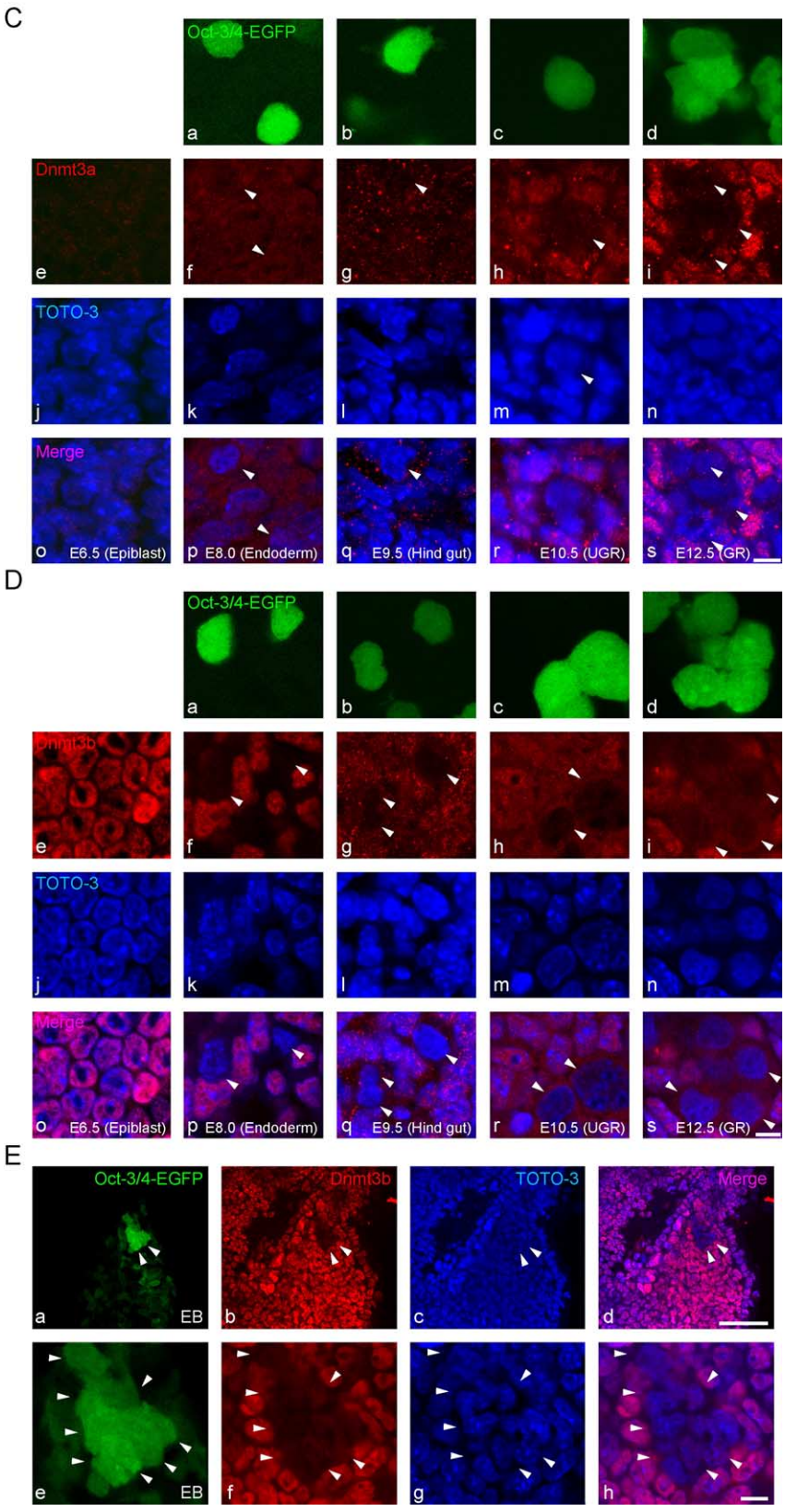

Fig. 3 (*continued*).

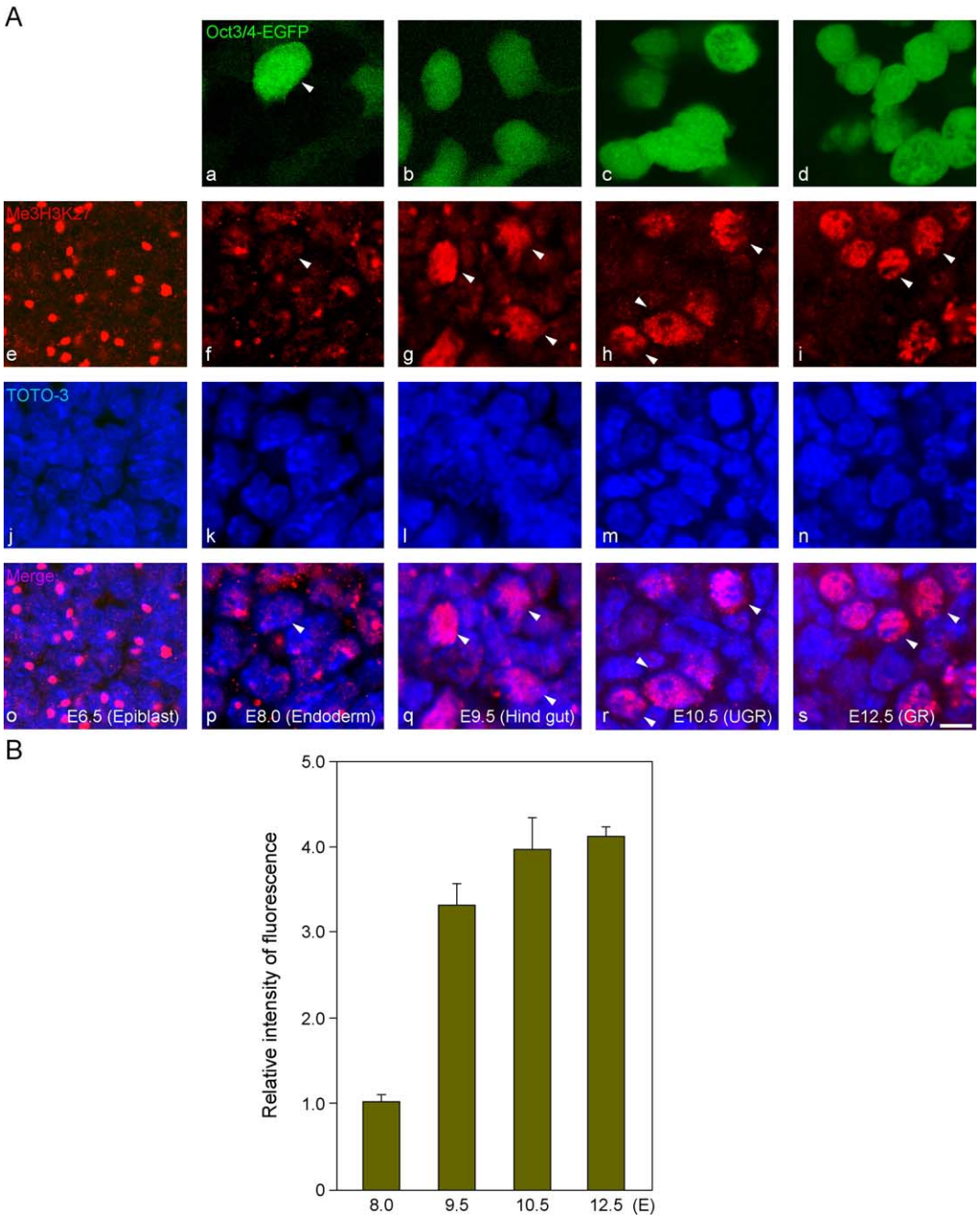

Fig. 4. H3-K27 trimethylation states in developing germ cells compared to those in surrounding somatic cells. (A) The levels of H3-K27 trimethylation are significantly elevated in germ cells at E8.5–9.0, and remain high until E12.5. Oct4ΔPE:GFP^{+} transgenic embryos at E6.5 (e, j, o), 8.0 (a, f, k, p), 9.5 (b, g, l, q), 10.5 (c, h, m, r), and 12.5 (d, i, n, s) stained with anti trimethylated H3-K27 antibody (red, e–i) and TOTO-3 (blue, j–n). GFP-positive cells (green, a–d) represent germ cells. Merged images of trimethylated H3-K27 and TOTO-3 staining are shown in (o–s). Note the significant up-regulation of H3-K27 trimethylation levels in germ cells at E9.5 (g). Arrowheads indicate germ cells. Scale bar in (s), 10 μm. (B) Semiquantification of H3-K27 trimethylation levels in developing germ cells compared to those in neighboring somatic cells. The intensity of fluorescent signals was quantified as described in Materials and methods. The average value for 10 somatic cells at each stage was set as 1.0.

positive germ cells did not consistently show. The weak, overall nuclear signals in germ cells were comparable to those of somatic cells. However, strikingly, in E9.5 germ cells, we detected very intense H3-K27 staining that was apparently more concentrated on euchromatic regions and less obvious in TOTO-3 strongly positive centromeric heterochromatic foci (Fig. 4Ab,g,l,q). This characteristic distribution was maintained until at least up to E12.5 (Fig. 4Ac,d,h,i). E9.5 germ cells occasionally showed single large spotted signals (Fig. 4Ag), which were presumably marking the inactive X chromosomes, which were also rarely observed at E12.5 (Fig. 4Ai). In contrast, the overall

nuclear H3-K27 trimethylation level in somatic cells remained low and single spotted signals were also progressively lost (Fig. 4Ai). These observations indicate that in somatic cells, H3-K27 trimethylation is confined mainly to an X chromosome undergoing an initial phase of inactivation, whereas in germ cells, this repressive modification covers entire euchromatic regions at very high levels from E8.5–9.0.

To confirm these findings, we collected E12.5 male and female germ and somatic cells from genital ridges using FACS or magnetic beads, as well as epiblast cells for western blot analysis. Consistent with our immunohistochemical analyses, the level of dimethylated H3-K9 in germ cells was found to be substantially lower than in somatic cells, whereas the levels of H3-K27 trimethylation were significantly higher in germ cells (Figs. 5A,B). These data strongly support the validity of the immunohistochemical procedure for the semiquantification of the antigen of interest.

Taken together, these findings clearly demonstrate that germ cells switch their genome-wide repressive mechanism on euchromatic regions from a H3-K9 dimethylated/DNA methylated state to a H3-K27 trimethylated state at E8.5–9.0. This might be linked to the reacquisition of the epigenetic plasticity of germ line genome.

H3-K4 methylation and H3-K9 acetylation; transcriptionally permissive germ cell nuclei

H3-K4 methylation and H3-K9 acetylation are typically coupled to transcriptionally permissive/active chromatin, and these two modifications mutually exclude H3-K9 methylation (Jenuwein and Allis, 2001). We therefore next examined the distribution of these two epigenetic markers. In E8.0 germ cells, as well as in proximal epiblast cells, H3-K4 methylation was found to localize throughout the euchromatic areas with many small foci but was largely absent from TOTO-3 positive centromeric heterochromatin and nucleoli (Fig. 6Aa,e,f,o,p). Nearby somatic cells exhibited similar staining patterns and the level of fluorescence was also relatively comparable between germ cells and somatic cells (Fig. 6B). This was also true at

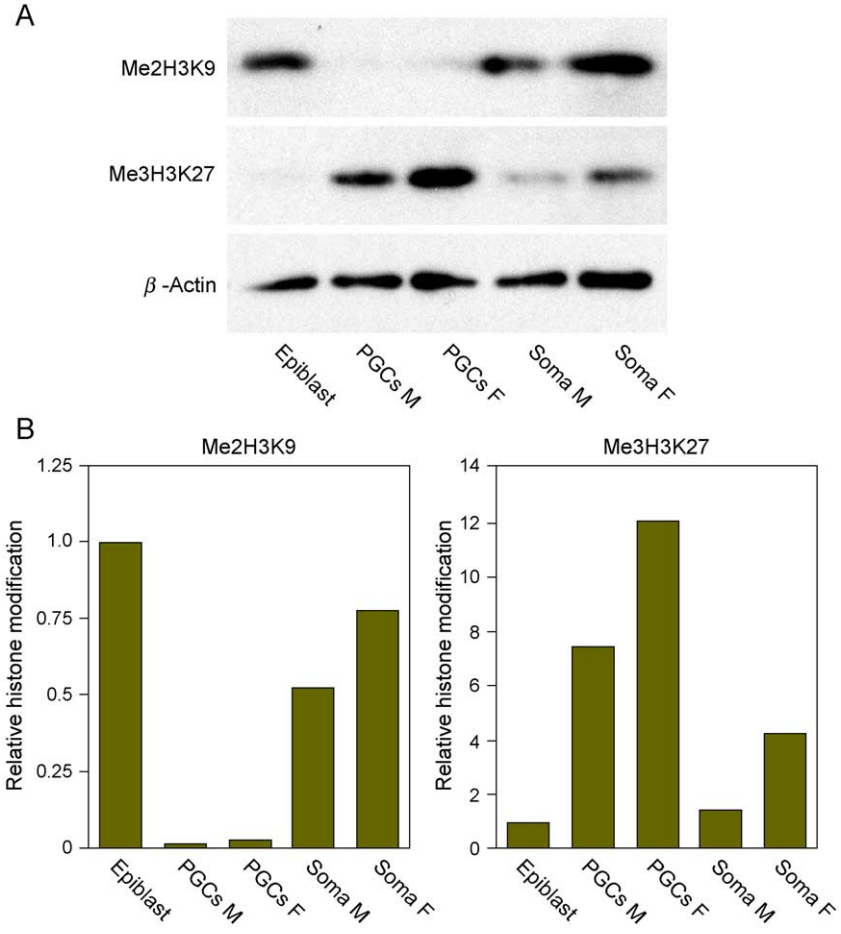

Fig. 5. Western blot analysis of H3-K9 dimethylation and H3-K27 trimethylation levels in germ cells compared to surrounding somatic cells at E12.5. (A) The levels of H3-K9 dimethylation and H3-K27 trimethylation were compared between epiblast cells at E6.5 and male and female germ and somatic cells at E12.5 by Western blot analyses. M denotes male and F denotes female. (B) Semiquantification of H3-K9 dimethylation and H3-K27 trimethylation levels in epiblast cells at E6.5, male and female germ and somatic cells at E12.5. The relative value for epiblast was set as 1.0. M denotes male and F denotes female.

E9.5 (Fig. 6Ab,g) but interestingly, at E10.5 germ cells specifically showed much higher fluorescence in comparison to surrounding gonadal somatic cells, although the signal distribution itself appeared indistinguishable (Figs. 6Ac,h and B). At E12.5, the level of H3-K4 methylation seemed again similar in germ cells and somatic cells (Figs. 6Ad,i and B). Analysis of H3-K9 acetylation revealed very similar distribution to H3-K4 methylation (Fig. 6C); E10.5 germ cells were also found to have much higher staining than surrounding somatic cells (Figs. 6Cc,h and D). These data indicate that germ cells have transcriptionally permissive/active chromatin, which is relatively similar to that in somatic cells during the migratory period, but as germ cells enter the genital ridge they transiently establish a hyperactive chromatin pattern.

Centromeric heterochromatin is relatively maintained in germ cells

We next analyzed H3-K9 trimethylation, a modification that specifically marks centromeric heterochromatin (Peters et al., 2003). Staining of proximal epiblast cells revealed H3-K9 trimethylation signals that were almost exclusively concentrated at several foci which consistently colocalized with TOTO-3 positive centromeric heterochromatin (Fig. 7e,j,o). At E8.0, GFP-labeled germ cells showed similar H3-K9 trimethylation foci (Fig. 7a,f). Although germ cells seemed to show somewhat lower signals (Fig. 7B), the overall appearance of H3-K9 trimethylation distribution in germ and neighboring somatic cells was relatively similar up to E12.5. We then examined the distribution of HP1α, a protein that binds methylated H3-K9 with high affinity and leads to heterochromatin formation (Jacobs and Khorasanizadeh, 2002; Lachner et al., 2001). In proximal epiblast cells, HP1α showed distinct concentration at TOTO-3-positive centromeric heterochromatin, as well as wide distribution in the nuclei, presumably reflecting dispersed localizations of H3-K9 methylated repressed regions on euchromatic arms (Fig. 7Ce,j,o). At E8.0, GFP-positive germ cells also showed clear concentration at heterochromatic foci and overall low level staining on euchromatin (Fig. 7Ca,f). Interestingly, after E9.5, the HP1α signal that located on presumptive euchromatic regions looked substantially decreased (Fig. 7Cb–d,g–i), and although the concentration on centromeric heterochromatin was relatively maintained, the overall level of HP1α signal in germ cells appeared lower than that in somatic cells (Fig. 7D). These observations are consistent with the idea that in germ cells HP1α remains concentrated on the centromeric heterochromatin that retain H3-K9 trimethylation but is removed from euchromatic arms that lose H3-K9 dimethylation and acquire H3-K27 trimethylation.

Collectively, these data demonstrate that within euchromatic regions germ cells erase a repressive mechanism operated by H3-K9 dimethylation and DNA methylation, and replace it with H3-K27 trimethylation, which is a modification that may allow greater nuclear plasticity. Transcriptionally permissive/active domains represented by H3-K4 methylation and H3-K9 acetylation are kept relatively constant but they appear to expand transiently when germ cells colonize the genital ridges. The structural integrity of centromeric heterochromatin created by H3-K9 trimethylation and HP1α are maintained relatively constant during early germ cell development, although the entire level of these modifications looks lower compared to those of somatic cells. This implies that the extensive epigenetic modifications occurring on germ cell euchromatin may partly influence those on the centromeres.

Discussion

We have provided evidence that early germ cells in mice undergo extensive genome-wide DNA demathylation and chromatin remodeling from soon after their birth in the extraembryonic mesoderm (Fig. 8). This epigenetic reprogramming might be necessary, as mouse germ cells arise from epiblast cells that are initially advancing toward a somatic cell fate (Saitou et al., 2002, 2003). Therefore, germ cell specification may initially necessitate the erasure of epigenetic modifications specific to somatic cell types and then the establishment of germ-line-specific modifications. This reprogramming appears to be precisely temporally coordinated and is probably controlled by an underlying genetic program, which is currently poorly understood.

We have shown that germ cells remove the majority of genome-wide H3-K9 dimethylation at around E8.0 (Fig. 1). This process appears to occur rapidly, as we observed that germ cells at the base of allantois exclusively displayed high levels of H3-K9 dimethylation, whereas migrating germ cells in the hindgut either exhibit high or low levels of methylation without exhibiting intermediate levels. Therefore, it appears that germ cells acquire a mechanism to swiftly and broadly erase this repressive modification from the genome during their early development. Interestingly, we found that at a similar stage, germ cells also largely remove DNA methylation from their genome (Fig. 2). This demethylation of DNA also seems to occur very rapidly. The timing and sequence of these two events seems to be well correlated, suggesting that these two events are mechanistically linked. Previous studies have reported that in *Neurospora crassa* and *Arabidopsis thaliana*, mutations in H3-K9 methyltransferases disrupt not only histone methylation but almost completely DNA methylation as well (Jackson et al., 2002; Tamaru and Selker, 2001). Furthermore, in mammalian cells, the methylase, Suv39h, is required for DNA methylation at pericentromeric heterochromatin (Lehnertz et al., 2003). In the fertilized oocyte, the paternal pronucleus is known to undergo active DNA demethylation that is preceded by the absence of H3-K9

dimethylation (Liu et al., 2004; Mayer et al., 2000; Oswald et al., 2000). These findings indicate that H3-K9 methylation is an upstream modification that controls DNA methylation. However, there are also reports demonstrating that methylated DNA can recruit histone methylation complexes, thereby acting as a key element in initiating

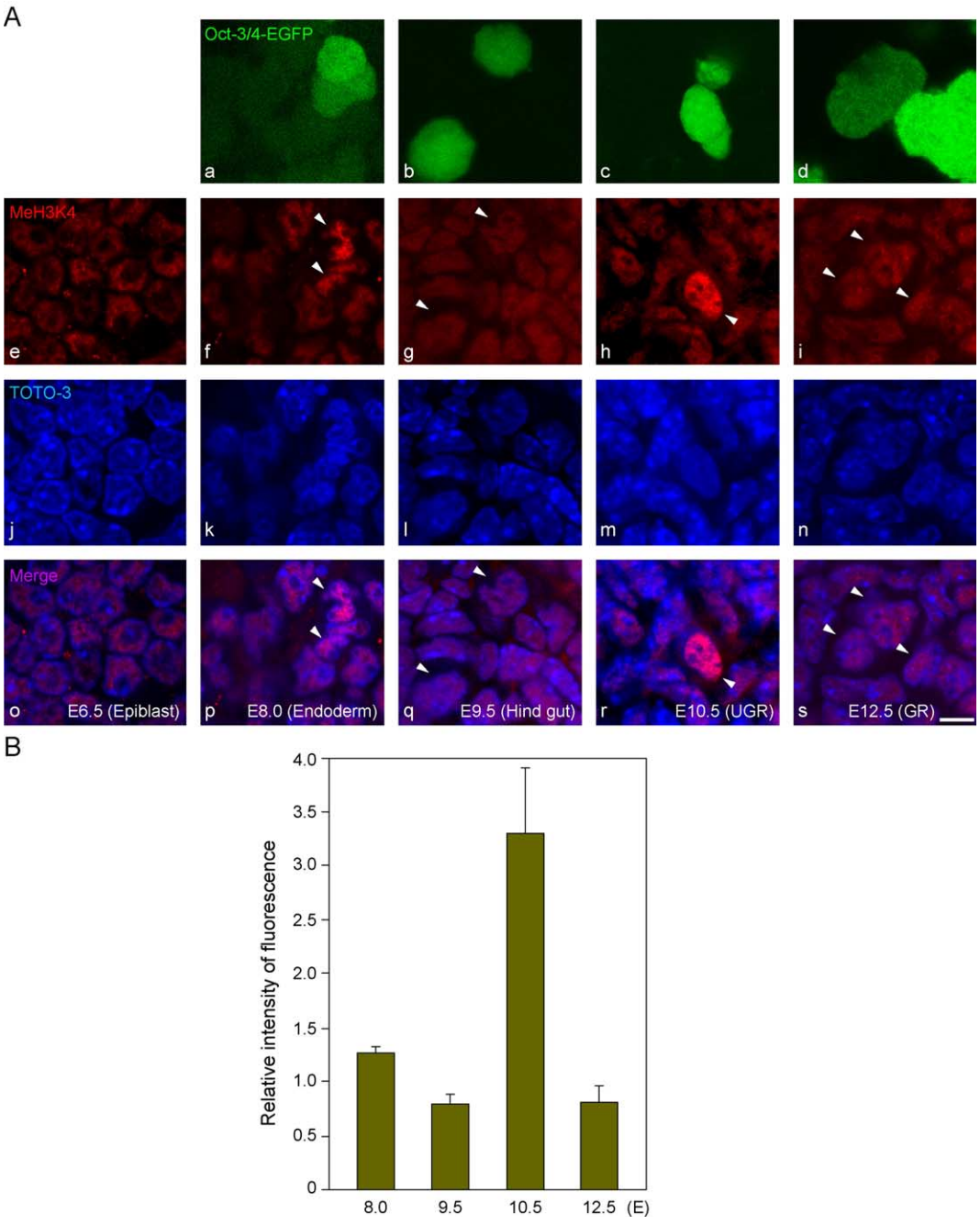

Fig. 6. H3-K4 methylation and H3-K9 acetylation states in developing germ cells compared to those in surrounding somatic cells. (A) The levels of both modifications are acutely elevated in germ cells upon their entry into genital ridges at E10.5. (A) Oct4ΔPE:GFP^{+} transgenic embryos at E6.5 (e, j, o), 8.0 (a, f, k, p), 9.5 (b, g, l, q), 10.5 (c, h, m, r) and 12.5 (d, i, n, s) stained with anti-methylated H3-K4 antibody (red, e–i) and TOTO-3 (blue, j–n). GFP-positive cells (green, a–d) represent germ cells. Merged images of methylated H3-K4 and TOTO-3 staining are shown in (o–s). Arrowheads indicate germ cells. Scale bar in (s), 10 μm. (B) Semiquantification of H3-K4 methylation levels in developing germ cells compared to those in neighboring somatic cells. The intensity of fluorescent signals was quantified as described in Materials and methods. The average value for ten somatic cells at each stage was set as 1.0. (C) Oct4ΔPE:GFP^{+} transgenic embryos at E6.5 (e, j, o), 8.0 (a, f, k, p), 9.5 (b, g, l, q), 10.5 (c, h, m, r) and 12.5 (d, i, n, s) stained with anti-acetylated H3-K9 antibody (red, e–i) and TOTO-3 (blue, j–n). GFP-positive cells (green, a–d) represent germ cells. Merged images of acetylated H3-K9 and TOTO-3 staining are shown in (o–s). Arrowheads indicate germ cells. Scale bar in (s), 10 μm. (D) Semiquantification of H3-K9 acetylation levels in developing germ cells compared to those in neighboring somatic cells. The intensity of fluorescent signals was quantified as described in Materials and methods. The average value for 10 somatic cells at each stage was set as 1.0.

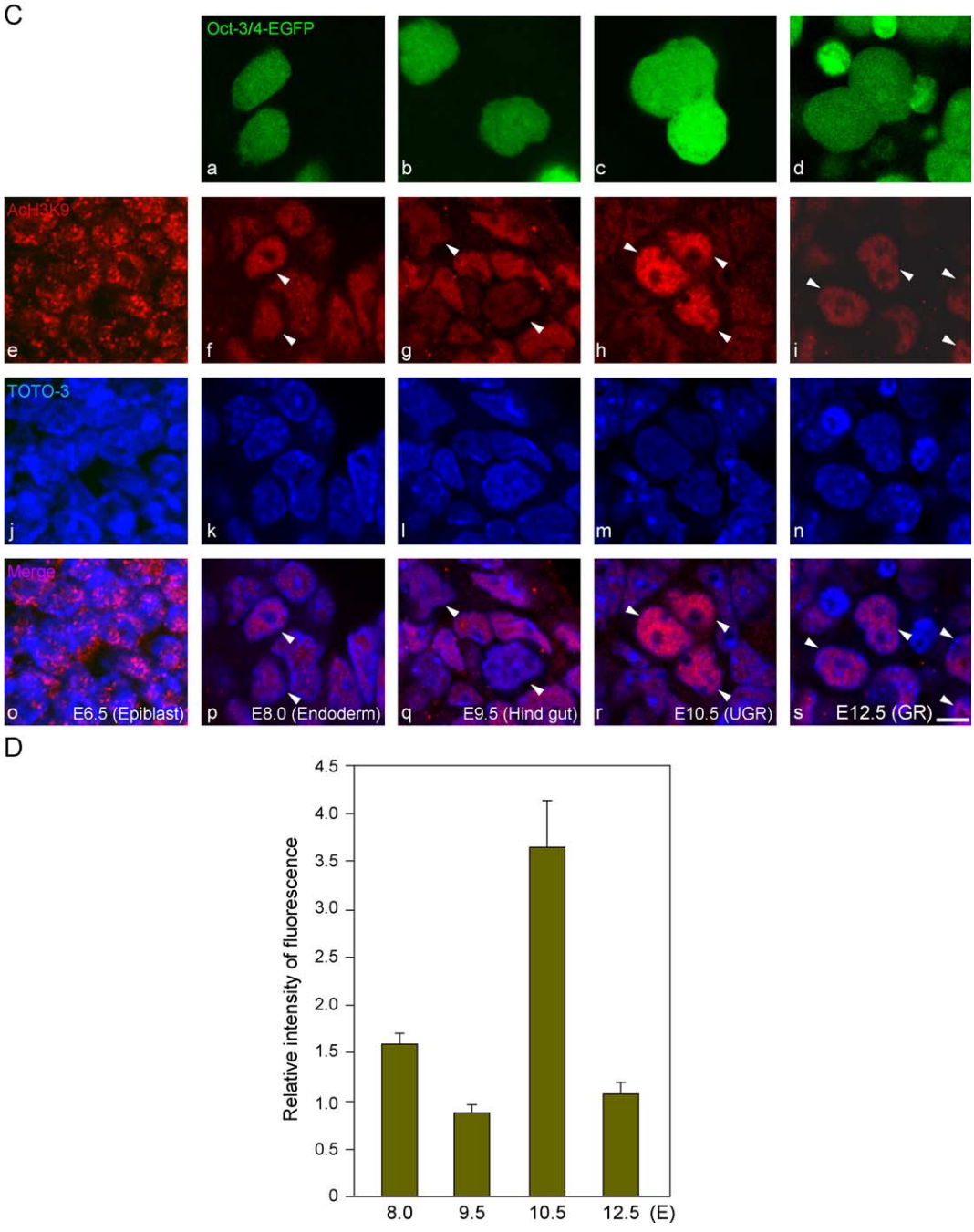

Fig. 6 (*continued*).

the creation of a repressive chromatin structure including H3-K9 dimethylation (Hashimshony et al., 2003; Fujita et al., 2003). Furthermore, a mutation in the DNA methyltransferase, MET1, in *Arabidopsis* results in the reduced level of H3-K9 dimethylation (Soppe et al., 2002). Therefore, apparently, DNA methylation can work as an upstream element of H3-K9 methylation in some cases. It is therefore important and necessary to determine precisely which event precedes the other in developing germ cells. We found that germ cells transiently down-regulate the expression of all the Dnmts before DNA demethylation takes place (Fig. 3). This seems to last approximately 16 h, which corresponds to the time required for one cell cycle in migrating germ cells (Tam and Snow, 1981). It would therefore be possible that replication-dependent loss of DNA methylation from a single strand may be triggering a cue for both loss of H3-K9 dimethylation and further DNA demethylation. In any case, it has became clear that early germ cells offer a good system

in which to explore the molecular mechanisms of histone and DNA demethylation, both of which present fundamental questions in epigenetic regulation.

We have also demonstrated that from about E8.5 germ cells strongly up-regulate H3-K27 trimethylation (Fig. 4) on their entire euchromatic region. H3-K27 trimethylation is another repressive modification mediated by Ezh2/Eed that is strongly associated with all the euchromatin in early blastomeres including the maternal pronucleus. Later, H3-K27 trimethylation is selectively maintained in the pluripotent inner cell mass, but in the trophectoderm it becomes exclusively concentrated on the inactive X chromosome

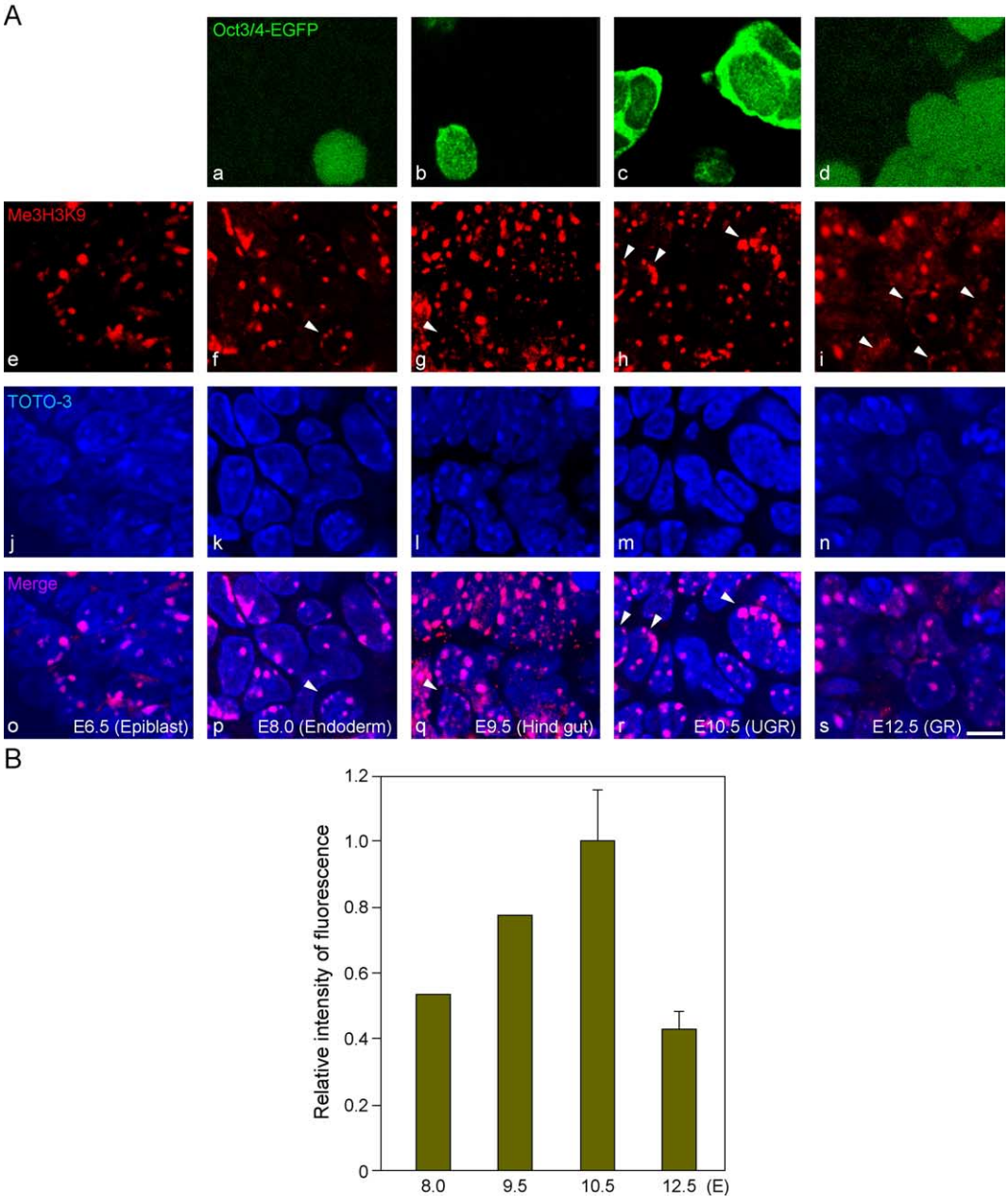

Fig. 7. H3-K9 trimethylation states and HP1α localization in developing germ cells compared to those in surrounding somatic cells. (A) Oct4ΔPE:GFP^{+} transgenic embryos at E6.5 (e, j, o), 8.0 (a, f, k, p), 9.5 (b, g, l, q), 10.5 (c, h, m, r) and 12.5 (d, i, n, s) stained with anti-trimethylated H3-K9 antibody (red, e–i) and TOTO-3 (blue, j–n). GFP-positive cells (green, a–d) represent germ cells. Merged images of trimethylated H3-K9 and TOTO-3 staining are shown in (o–s). Arrowheads indicate germ cells. Scale bar in (s), 10 μm. (B) Semiquantification of H3-K9 trimethylation levels in developing germ cells compared to those in neighboring somatic cells. The intensity of fluorescent signals was quantified as described in Materials and methods. The average value for ten somatic cells at each stage was set as 1.0. (C) Oct4ΔPE:GFP^{+} transgenic embryos at E6.5 (e, j, o), 8.0 (a, f, k, p), 9.5 (b, g, l, q), 10.5 (c, h, m, r) and 12.5 (d, i, n, s) stained with anti-HP1α antibody (red, e–i) and TOTO-3 (blue, j–n). GFP-positive cells (green, a–d) represent germ cells. Merged images of HP1α and TOTO-3 staining are shown in (o–s). Arrowheads indicate germ cells. Scale bar in (s), 10 μm. (D) Semiquantification of HP1α levels in developing germ cells compared to those in neighboring somatic cells. The intensity of fluorescent signals was quantified as described in Materials and methods. The average value for 10 somatic cells at each stage was set as 1.0.

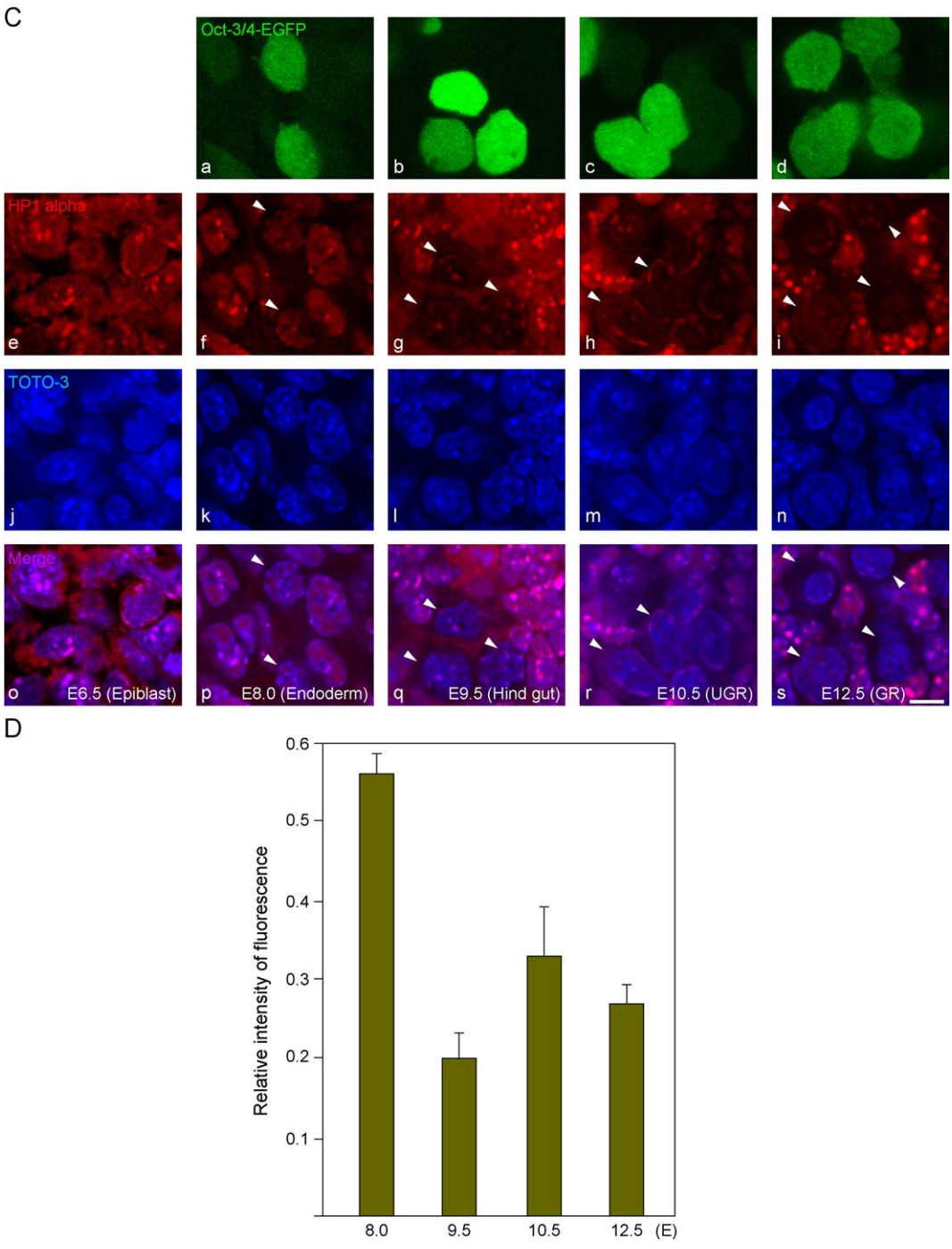

Fig. 7 (*continued*).

(Erhardt et al., 2003; Plath et al., 2003; Silva et al., 2003). Subsequently, also in the epiblast, euchromatic H3-K27 trimethylation is lost and this modification becomes accumulated only on the inactive X chromosome (Erhardt et al., 2003). Therefore, euchromatic H3-K27 trimethylation is apparently exploited for genome-wide repression in pluripotent cell lineages including early germ cells as well as during the initial phase of X chromosome inactivation. In this context, it is interesting to note that ES cells can be maintained in an undifferentiated state in the absence of Suv39h and G9a (Lehnertz et al., 2003; Tachibana et al., 2002), and associated centromeric H3-K9 trimethylation and euchromatic H3-K9 dimethylation, respectively, whereas the presence of Ezh2 and associated H3-K27 trimethylation is an absolute requirement for ES cell derivation and propagation (O'Carroll et al., 2001). It appears to be the case that

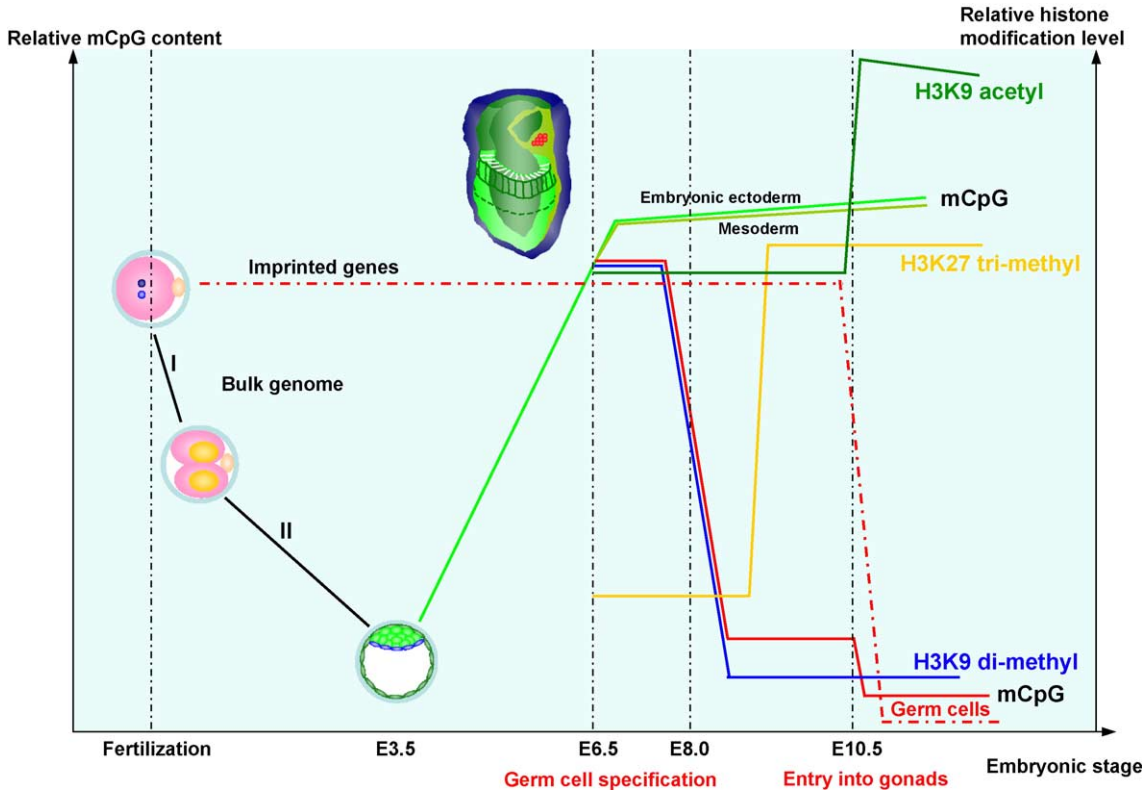

Fig. 8. Schematic representation of genome-wide reprogramming of chromatin modifications in germ cell development. The epigenetic remodeling occurring in germ cell development is shown in combination with that during the developmental period up to germ cell specification. Only DNA methylation behavior is shown for the early stages. After fertilization, the paternal genome undergoes active genome-wide DNA demethylation (I) that is followed by passive replication-dependent demethylation of both the paternal and maternal genomes after the two-cell stage (II), which continues until the morula stage by which time the genome-wide DNA methylation level has become very low. Imprinted genes escape this genome-wide DNA demethylation process. The genome-wide H3-K9 dimethylation level decreases in a similar manner, reaching the lowest state also at the eight-cell stage. Thereafter, in the pluripotent epiblast, Dnmt3a and 3b become active and the methylation levels in the epiblast cells increase rapidly, preparing for the differentiation of somatic lineages. Specified germ cells (E7.0) appear to retain DNA methylation and dimethylated H3-K9 levels similar to those in surrounding somatic cells. However, rapid genome-wide removal of these two modifications occurs specifically in germ cells at around E8.0. DNA methylation is further down-regulated in germ cells after their entry into genital ridges. In contrast, H3-K27 trimethylation levels, of which genome-wide levels are low in the epiblast, elevate sharply in germ cells at around E8.5 and are maintained until at least E12.5. In addition, the germ cell levels of H3-K4 methylation and H3-K9 acetylation are acutely and transiently up-regulated at E10.5, when germ cells enter into genital ridges.

compared to rather tightly packaged, stably repressed heterochromatin generated by H3-K9 dimethylation and DNA methylation, H3-K27 trimethylation creates a repressed but more plastic state of chromatin that may be able to respond to reprogramming cues more easily. Consistently, it has been shown that an early inactive X chromosome phase can be reversed when H3-K27 trimethylation is the major modification but X-inactivation becomes irreversible after H3-K9 is heavily dimethylated (Silva et al., 2003). Therefore, the transition of a euchromatic repression system consisting of H3-K9 dimethylation and DNA methylation to that consisting of H3-K27 trimethylation might herald the reacquisition of underlying totipotency in germ cells.

Compared to the substantial alterations of repressive modifications in their euchromatic regions, germ cells maintain H3-K9 trimethylation and associated HP1α localization at centromeric heterochromatin with relative constancy throughout their development, although their level appeared to be lower compared to neighboring somatic cells (Fig. 7). This may contribute to retaining the overall integrity of germ cell chromatin and chromosome structure while the genome is undergoing extensive epigenetic modifications. H3-K4 methylation and H3-K9 acetylation, both associated with transcriptionally active/permissive chromatin, are also relatively constant during germ cell migration but are both highly up-regulated as germ cells colonize the genital ridges (Fig. 6). When the transcriptional states were monitored by staining with anti-phospho serine2 of the C terminal domain of RNA polymerase II (H5 antibody), germ cells in the genital ridge showed similar intensity to that of somatic cells (data not shown). This data suggests that germ cell chromatin is highly decondensed in the genital ridges but is not necessarily transcriptionally hyperactive.

It is of importance to note that the chromatin modifications in early germ cells in mice described here are significantly different from those in *C. elegans* and *D.*

melanogaster (Schaner et al., 2003). In *C. elegans*, early germ line precursors are transcriptionally inactive. However, precursor blastomeres for germ cells (P1 to P3) that produce one germ line and one somatic descendant at each cell division exhibit transcriptionally permissive chromatin states with genome-wide high level H3-K4 methylation. This is presumably because these precursors still produce somatic cells that have to start somatic transcription soon after the cleavage (Seydoux and Strome, 1999). Transcriptional quiescence in these germ line precursors is instead maintained by the activity of germ-line-specific Zn finger protein, PIE-1, which apparently inhibits transcriptional elongation (Batchelder et al., 1999; Seydoux and Dunn, 1997). In contrast, the chromatin of the Z2 and Z3 cells that produce two germ line cells after cell division exhibit a transcriptionally inactive state with low levels of H3-K4 methylation. Thus, germ line precursors in *C. elegans* shift their chromatin states from a transcriptionally permissive to an inactive one at the P4 to Z2 and Z3 transition with concomitant degradation of PIE-1 protein. The germ line precursors in *D. melanogaster*, known as pole cells, are also transcriptionally inactive (Seydoux and Dunn, 1997). However, in contrast to *C. elegans*, their chromatin takes a transcriptionally inactive state at the outset with high levels of H3-K9 methylation (Schaner et al., 2003). This is probably because pole cells only produce germ line cells and thus are possibly epigenetically similar to P4 or Z2 and Z3 cells in *C. elegans*. We have demonstrated that germ cell chromatin in mice is intricately maintained in a dynamic balance of active (H3-K4 methylated/H3-K9 acetylated) and plastically repressive (H3-K27 trimethylated) states. Increased complexity of epigenetic regulation in mice that include the acquisition of parental imprinting and a substantially different mode of early development and germ cell specification may be responsible for these differences.

Recent studies have shown that both oocytes and sperm can be derived from ES cells in vitro (Geijsen et al., 2004; Hubner et al., 2003; Toyooka et al., 2003). However, it remains unclear if these in vitro germ cells acquire appropriate epigenotypes necessary for the successful production of their progeny. Our study revealed that germ cells in vivo undergo extensive yet highly ordered genome-wide epigenetic reprogramming during their early development. Perturbation of some of these processes may lead to the formation of apparently morphologically 'normal' germ cells but which contain inappropriate epigenotypes that may produce gametes resulting in aberrant development. Therefore, it is important to understand the essential molecular mechanisms controlling epigenetic development of normal in vivo germ cells in order to fully understand and direct germ cell development in vitro. Considering that epigenetic reprogramming in early germ cells occurs in a highly ordered way during relatively a short period of time, germ cells may acquire an intrinsic molecular program, which establishes this epigenetic program when they are first specified.

Acknowledgments

We thank Drs. S. Tajima and I. Suetake for Dnmt antibodies, and P. Western and K. Una for critically reading the manuscript. This work was supported in part by the Science and Technology Agency of Japan, with Special Coordinating Funds of Promoting Science and Technology, by CREST of JST (Japan Science and Technology Corporation), by grants-in-aid from the Ministry of Education, Science, Sports and Culture of Japan.

References

Anderson, R., Copeland, T.K., Scholer, H., Heasman, J., Wylie, C., 2000. The onset of germ cell migration in the mouse embryo. Mech. Dev. 91, 61–68.

Arney, K.L., Bao, S., Bannister, A.J., Kouzarides, T., Surani, M.A., 2002. Histone methylation defines epigenetic asymmetry in the mouse zygote. Int. J. Dev. Biol. 46, 317–320.

Batchelder, C., Dunn, M.A., Choy, B., Suh, Y., Cassie, C., Shim, E.Y., Shin, T.H., Mello, C., Seydoux, G., Blackwell, T.K., 1999. Transcriptional repression by the *Caenorhabditis elegans* germ-line protein PIE-1. Genes Dev. 13, 202–212.

Bird, A., 2002. DNA methylation patterns and epigenetic memory. Genes Dev. 16, 6–21.

Erhardt, S., Su, I.H., Schneider, R., Barton, S., Bannister, A.J., Perez-Burgos, L., Jenuwein, T., Kouzarides, T., Tarakhovsky, A., Surani, M.A., 2003. Consequences of the depletion of zygotic and embryonic enhancer of zeste 2 during preimplantation mouse development. Development 130, 4235–4248.

Fujita, N., Watanabe, S., Ichimura, T., Tsuruzoe, S., Shinkai, Y., Tachibana, M., Chiba, T., Nakao, M., 2003. Methyl-CpG binding domain 1 (MBD1) interacts with the Suv39h1-HP1 heterochromatic complex for DNA methylation-based transcriptional repression. J. Biol. Chem. 278, 24132–24138 (Electronic publication 2003 Apr. 23).

Geijsen, N., Horoschak, M., Kim, K., Gribnau, J., Eggan, K., Daley, G.Q., 2004. Derivation of embryonic germ cells and male gametes from embryonic stem cells. Nature 427, 148–154.

Ginsburg, M., Snow, M.H., McLaren, A., 1990. Primordial germ cells in the mouse embryo during gastrulation. Development 110, 521–528.

Hajkova, P., Erhardt, S., Lane, N., Haaf, T., El-Maarri, O., Reik, W., Walter, J., Surani, M.A., 2002. Epigenetic reprogramming in mouse primordial germ cells. Mech. Dev. 117, 15–23.

Hashimshony, T., Zhang, J., Keshet, I., Bustin, M., Cedar, H., 2003. The role of DNA methylation in setting up chromatin structure during development. Nat. Genet. 34, 187–192.

Holdeman, R., Nehrt, S., Strome, S., 1998. MES-2, a maternal protein essential for viability of the germline in *Caenorhabditis elegans*, is homologous to a *Drosophila* Polycomb group protein. Development 125, 2457–2467.

Hubner, K., Fuhrmann, G., Christenson, L.K., Kehler, J., Reinbold, R., De La Fuente, R., Wood, J., Strauss, I.J., Boiani, M., Scholer, H.R., 2003. Derivation of oocytes from mouse embryonic stem cells. Science 1, 1.

Jackson, J.P., Lindroth, A.M., Cao, X., Jacobsen, S.E., 2002. Control of CpNpG DNA methylation by the KRYPTONITE histone H3 methyltransferase. Nature 416, 556–560.

Jacobs, S.A., Khorasanizadeh, S., 2002. Structure of HP1 chromodomain bound to a lysine 9-methylated histone H3 tail. Science 295, 2080–2083.

Jenuwein, T., Allis, C.D., 2001. Translating the histone code. Science 293, 1074–1080.

Lachner, M., O'Carroll, D., Rea, S., Mechtler, K., Jenuwein, T., 2001.

Methylation of histone H3 lysine 9 creates a binding site for HP1 proteins. Nature 410, 116–120.
Lachner, M., O'Sullivan, R.J., Jenuwein, T., 2003. An epigenetic road map for histone lysine methylation. J. Cell Sci. 116, 2117–2124.
Lane, N., Dean, W., Erhardt, S., Hajkova, P., Surani, A., Walter, J., Reik, W., 2003. Resistance of IAPs to methylation reprogramming may provide a mechanism for epigenetic inheritance in the mouse. Genesis 35, 88–93.
Lawson, K.A., Hage, W.J., 1994. Clonal analysis of the origin of primordial germ cells in the mouse. Ciba Found. Symp. 182, 68–84 (Discussion 84–91).
Lawson, K.A., Dunn, N.R., Roelen, B.A., Zeinstra, L.M., Davis, A.M., Wright, C.V., Korving, J.P., Hogan, B.L., 1999. Bmp4 is required for the generation of primordial germ cells in the mouse embryo. Genes Dev. 13, 424–436.
Lehnertz, B., Ueda, Y., Derijck, A.A., Braunschweig, U., Perez-Burgos, L., Kubicek, S., Chen, T., Li, E., Jenuwein, T., Peters, A.H., 2003. Suv39h-mediated histone H3 lysine 9 methylation directs DNA methylation to major satellite repeats at pericentric heterochromatin. Curr. Biol. 13, 1192–1200.
Li, E., 2002. Chromatin modification and epigenetic reprogramming in mammalian development. Nat. Rev., Genet. 3, 662–673.
Li, E., Bestor, T.H., Jaenisch, R., 1992. Targeted mutation of the DNA methyltransferase gene results in embryonic lethality. Cell 69, 915–926.
Liu, H., Kim, J.M., Aoki, F., 2004. Regulation of histone H3 lysine 9 methylation in oocytes and early pre-implantation embryos. Development 131, 2269–2280 (Electronic publication 2004 Apr. 21).
Mayer, W., Niveleau, A., Walter, J., Fundele, R., Haaf, T., 2000. Demethylation of the zygotic paternal genome. Nature 403, 501–502.
Molyneaux, K.A., Stallock, J., Schaible, K., Wylie, C., 2001. Time-lapse analysis of living mouse germ cell migration. Dev. Biol. 240, 488–498.
O'Carroll, D., Erhardt, S., Pagani, M., Barton, S.C., Surani, M.A., Jenuwein, T., 2001. The polycomb-group gene Ezh2 is required for early mouse development. Mol. Cell. Biol. 21, 4330–4336.
Okano, M., Bell, D.W., Haber, D.A., Li, E., 1999. DNA methyltransferases Dnmt3a and Dnmt3b are essential for de novo methylation and mammalian development. Cell 99, 247–257.
Oswald, J., Engemann, S., Lane, N., Mayer, W., Olek, A., Fundele, R., Dean, W., Reik, W., Walter, J., 2000. Active demethylation of the paternal genome in the mouse zygote. Curr. Biol. 10, 475–478.
Pesce, M., De Felici, M., 1995. Purification of mouse primordial germ cells by MiniMACS magnetic separation system. Dev. Biol. 170, 722–725.
Peters, A.H., O'Carroll, D., Scherthan, H., Mechtler, K., Sauer, S., Schofer, C., Weipoltshammer, K., Pagani, M., Lachner, M., Kohlmaier, A., Opravil, S., Doyle, M., Sibilia, M., Jenuwein, T., 2001. Loss of the Suv39h histone methyltransferases impairs mammalian heterochromatin and genome stability. Cell 107, 323–337.
Peters, A.H., Kubicek, S., Mechtler, K., O'Sullivan, R.J., Derijck, A.A., Perez-Burgos, L., Kohlmaier, A., Opravil, S., Tachibana, M., Shinkai, Y., Martens, J.H., Jenuwein, T., 2003. Partitioning and plasticity of repressive histone methylation states in mammalian chromatin. Mol. Cell 12, 1577–1589.
Plath, K., Fang, J., Mlynarczyk-Evans, S.K., Cao, R., Worringer, K.A., Wang, H., de la Cruz, C.C., Otte, A.P., Panning, B., Zhang, Y., 2003. Role of histone H3 lysine 27 methylation in X inactivation. Science 300, 131–135.
Rougier, N., Bourc'his, D., Gomes, D.M., Niveleau, A., Plachot, M., Paldi, A., Viegas-Pequignot, E., 1998. Chromosome methylation patterns during mammalian preimplantation development. Genes Dev. 12, 2108–2113.
Saitou, M., Barton, S.C., Surani, M.A., 2002. A molecular programme for the specification of germ cell fate in mice. Nature 418, 293–300.
Saitou, M., Payer, B., Lange, U.C., Erhardt, S., Barton, S.C., Surani, M.A., 2003. Specification of germ cell fate in mice. Philos. Trans. R. Soc. Lond., B Biol. Sci. 358, 1363–1370.
Sakai, Y., Suetake, I., Itoh, K., Mizugaki, M., Tajima, S., Yamashina, S., 2001. Expression of DNA methyltransferase (Dnmt1) in testicular germ cells during development of mouse embryo. Cell Struct. Funct. 26, 685–691.
Sanford, J., Forrester, L., Chapman, V., Chandley, A., Hastie, N., 1984. Methylation patterns of repetitive DNA sequences in germ cells of *Mus musculus*. Nucleic Acids Res. 12, 2823–2836.
Sato, S., Yoshimizu, T., Sato, E., Matsui, Y., 2003. Erasure of methylation imprinting of Igf2r during mouse primordial germ-cell development. Mol. Reprod. Dev. 65, 41–50.
Schaner, C.E., Deshpande, G., Schedl, P.D., Kelly, W.G., 2003. A conserved chromatin architecture marks and maintains the restricted germ cell lineage in worms and flies. Dev. Cell 5, 747–757.
Seydoux, G., Dunn, M.A., 1997. Transcriptionally repressed germ cells lack a subpopulation of phosphorylated RNA polymerase II in early embryos of *Caenorhabditis elegans* and *Drosophila melanogaster*. Development 124, 2191–2201.
Seydoux, G., Strome, S., 1999. Launching the germline in *Caenorhabditis elegans*: regulation of gene expression in early germ cells. Development 126, 3275–3283.
Silva, J., Mak, W., Zvetkova, I., Appanah, R., Nesterova, T.B., Webster, Z., Peters, A.H., Jenuwein, T., Otte, A.P., Brockdorff, N., 2003. Establishment of histone h3 methylation on the inactive X chromosome requires transient recruitment of Eed-Enx1 polycomb group complexes. Dev. Cell 4, 481–495.
Soppe, W.J., Jasencakova, Z., Houben, A., Kakutani, T., Meister, A., Huang, M.S., Jacobsen, S.E., Schubert, I., Fransz, P.F., 2002. DNA methylation controls histone H3 lysine 9 methylation and heterochromatin assembly in *Arabidopsis*. EMBO J. 21, 6549–6559.
Surani, M.A., 2001. Reprogramming of genome function through epigenetic inheritance. Nature 414, 122–128.
Tachibana, M., Sugimoto, K., Nozaki, M., Ueda, J., Ohta, T., Ohki, M., Fukuda, M., Takeda, N., Niida, H., Kato, H., Shinkai, Y., 2002. G9a histone methyltransferase plays a dominant role in euchromatic histone H3 lysine 9 methylation and is essential for early embryogenesis. Genes Dev. 16, 1779–1791.
Tam, P.P., Snow, M.H., 1981. Proliferation and migration of primordial germ cells during compensatory growth in mouse embryos. J. Embryol. Exp. Morphol. 64, 133–147.
Tam, P.P., Zhou, S.X., Tan, S.S., 1994. X-chromosome activity of the mouse primordial germ cells revealed by the expression of an X-linked lacZ transgene. Development 120, 2925–2932.
Tamaru, H., Selker, E.U., 2001. A histone H3 methyltransferase controls DNA methylation in *Neurospora crassa*. Nature 414, 277–283.
Toyooka, Y., Tsunekawa, N., Akasu, R., Noce, T., 2003. Embryonic stem cells can form germ cells in vitro. Proc. Natl. Acad. Sci. U. S. A. 100, 11457–11462 (Electronic publication 2003 Sep 22).
Watanabe, D., Suetake, I., Tada, T., Tajima, S., 2002. Stage- and cell-specific expression of Dnmt3a and Dnmt3b during embryogenesis. Mech. Dev. 118, 187–190.
Yoder, J.A., Walsh, C.P., Bestor, T.H., 1997. Cytosine methylation and the ecology of intragenomic parasites. Trends Genet. 13, 335–340.
Yoshimizu, T., Sugiyama, N., De Felice, M., Yeom, Y.I., Ohbo, K., Masuko, K., Obinata, M., Abe, K., Scholer, H.R., Matsui, Y., 1999. Germline-specific expression of the Oct-4/green fluorescent protein (GFP) transgene in mice. Dev. Growth Differ. 41, 675–684.